

# CORROSION OF WELD AREA AT INTERNAL SURFACE OF PIPELINE USED IN OIL AND GAS INDUSTRY

M.A. Azam<sup>1</sup>, M.F. Abdullah<sup>1</sup> and T. Shimoda<sup>2</sup>

<sup>1</sup>Faculty of Manufacturing Engineering,  
Universiti Teknikal Malaysia Melaka, Hang Tuah Jaya, 76100 Durian  
Tunggal, Melaka, Malaysia.

<sup>2</sup>School of Materials Science,  
Japan Advanced Institute of Science and Technology, Asahidai,  
Nomi, 923-1292 Ishikawa, Japan.

Corresponding Author's Email: <sup>1</sup>asyadi@utem.edu.my

**Article History:** Received 23 October 2019; Revised 14 March 2020;  
Accepted 24 October 2020

**ABSTRACT:** The objective of this work was to investigate the cause of failed pipeline steel, in particular at its weld area which may due to the preferential corrosion. The pipeline sample was supplied by an industry based in Miri, Sarawak. The serious circumstances in the piping scheme led to high-level corrosion of the inner surface, particularly in the weld region. Inside the pipe system, natural gas flowed into the processing operation within the platform. Several tests and experiments were elucidated to comprehend the metallographic of the failure portion in order to explore the failure. Pipe sample testing techniques such as visual inspection, optical microscope, scanning electron microscope, and Vickers hardness testing were carried out effectively. The characterization of the microstructure was carried out on the sample taken from three main regions of the sample, which are the base metal, the heat affected area and also the weld joint, in order to elaborate the difference of the properties. The test outcome has shown that corrosion occurred at the pipe, even though the pipe system used cathodic protection.

**KEYWORDS:** *Corrosion Failure Analysis; Carbon Steel; Weldment Area; Heat Affected Zone (HAZ)*

## 1.0 INTRODUCTION

Corrosion failure of weldment area of pipeline occurred through several facts such as the appropriate base metal, filler metal that has been selected, industry codes and also standards. Additionally, welds that have full weld penetration and correct shape and contour have been placed [1]. All the requirements have been followed but in a certain place and condition, the corrosion failures of weld still occur. It is not unusual things where the wrought form of a metal or alloy is resistant to corrosion in a particular environment, but the welded counterpart is not [2-3]. Generally, farther welds can be done with the addition of filler metal or perhaps can be produced autogenously or without having any consumption of filler metal. There are, however, some factors that may also affect the situation if the weld demonstrates superior corrosion resistance to the unwelded base metal [4]. In fact, there are moments when the weld responds erratically, indicating both strength and susceptibility to corrosive attacks [5].

Welding failure can be split into two groups; those dismissed after inspection and mechanical testing, and service errors that could occur due to corrosion, wear, fracture, or possibly deformation. Causes for rejection during inspection can be either noticeable on the welding surface or underground signs that can be identified using non-destructive test methods [6]. Service of the welds is same to that of some other components; are relying on the operating environment as well as the nature of the applied load [7]. It may also include errors such as brittle cracking, ductile cracking overload failure, plastic collapse, buckling fatigue, corrosion, stress-corrosion cracking, and hydrogen cracking.

In the case of elevated temperatures, creep deformation and stress rupture must be considered [8]. Typically, ductile fracture, plastic collapse and buckling are preceded by plastic deformation which could give some warning or indication before the final fracture [9]. In contrast, the spread of brittle crack is preceded by negligible deformation and can lead without warning to fast erratic crack development and catastrophic failure. Break fracture of welded systems is rare; however, it can be exaggerated, frequently resulting in serious conditions [10].

As the corrosion failure of weldment stated above, a study and failure analysis is conducted in order to find the cause of the failure of the carbon steel pipeline which has been supplied by the industry.

## 2.0 METHODOLOGY

### 2.1 Data Collection and Visual Inspection

Data collection for the pipe sample was performed to ensure what type of corrosion happened in the internal surface of the sample. The concepts and explanations of the corrosion have been correlated with the data, information and in-service history of the pipe. Visual inspection carried out in order to evaluate detail surface damage and preparing the analysis and investigation plan for sample of line 350-PG-2406-61490X of weld no 01, which shows root defect. The conditions of root part especially weld circumference shows of Preferential Weld Corrosion. The internal surface of the weld shows brown color. The working conditions for the pipeline are tabulated in Table 1.

Table 1: The working conditions for the pipeline

Parameter	Features
Piping Line No	350-PG-2406-61490X
Sample name	HIP (Weld no 1)
Type	14" Low Pressure Discharge Line
Material	14" Schedule 80
Operating Pressure (Bar g)	53
Years in service	7 to 8 years
Joint Type	Single V

Optical microscope (OM) used to evaluate and identify microstructure deference in each of weld. The metallographic observation of materials represents the wide selection of features which can be assessed by OM. In this examination, it is more focused on 3 areas at both (right side and left side). It was heat affected zone (HAZ) end, parent metal and weld metal.

Scanning electron microscope (SEM) was used with the scale of 3- $\mu$ m and 10- $\mu$ m, high magnification of 1000 X in order to detect changes in micro scale [11]. By SEM, the type of failures can be identified closely and specifically. For this examination, SEM only focused at weld area (hot pass) and HAZ, in order to find any failure in term of weld discontinuities such as pitting, crack, slag or porosity.

Vickers hardness test was carried out to observe material ability to resist plastic deformation [12]. Besides that, it also meant to identify the hardness distribution value at the sample where hardness can be related to the microstructure properties that occur after metallographic examination. The load duration was set in 15 seconds and the sample was placed under the test load of 0.1 N. Then under the magnification of 50 x objective lens, the reading of the diamond shape at the material is taken.

## **2.2 Sample Preparation**

The area of the sample which is of interest needs to be sectioned from the pipe. Any single sample need to be mounted to control and facilitate handling. The specimen was cut from the pipe samples. The characterization of the microstructure was carried out from three primary areas of the weld in order to compare helpful characteristics.

Mounting facilitates controlling and handling of the specimen. For this sample mounting preparation, the technique used was cold mounting. The polyvinyl chloride (PVC) pipe with inner diameter of 60 mm and 12.5 mm height was use as a mold. 200 g of polyester and ½ spoon of methyl ethyl ketone peroxide (MEKP) was poured in the mold. Then the sample was set at room temperature and left for 24 hours.

Grinding was carried out with a sequence of grit paper starting from 240, 400, 600, 800 and finally 1200 grits before the microstructural analysis. Grinding speed required was around 150 to 200 rpm, where this speed will give good contact between the sample and abrasive paper. The time required for the grinding process is only about 2 to 3 minutes for each type abrasive paper.

The samples were polished by fine polishing cloth. Fine polishing process is conducted using the cloth covering on top of impregnated wheel. Polishing can remove scratches or residual defects when cutting metal. For this sample, the speed grinding speed required is around 200-250 rpm. By using alumina solution, time required for polishing process is around 5 minutes.

Etching was performed to reveal the microstructure of the corrosion product at grain boundaries [13]. Etching also includes any sort of process utilized to reveal the microstructure of the sample. The sample was immersed in an etchant solution. The etching process was done to the sample with the usage of Nital 3%, 5 ml Nitric acid plus 100 ml ethanol.

## **3.0 RESULTS AND DISCUSSION**

### **3.1 Visual Inspection**

For inner surface, thin preferential severe corrosion was observed at all length of weld with 8.9 to 12.0 mm depth. Thin preferential corrosion was observed at both HAZ area, with the 0.8 to 0.9 mm depth, along

the line of flow. It is located at 15 mm to 20 mm width, at both upper stream side and downstream side. At downstream side, thin layer corrosion is scattered was observed, which is 75 mm from the weld, with the depth of 0.3 to 0.8 mm, along the line of flow. Schematic illustration in Figure 1 shows the inner side of the pipe.

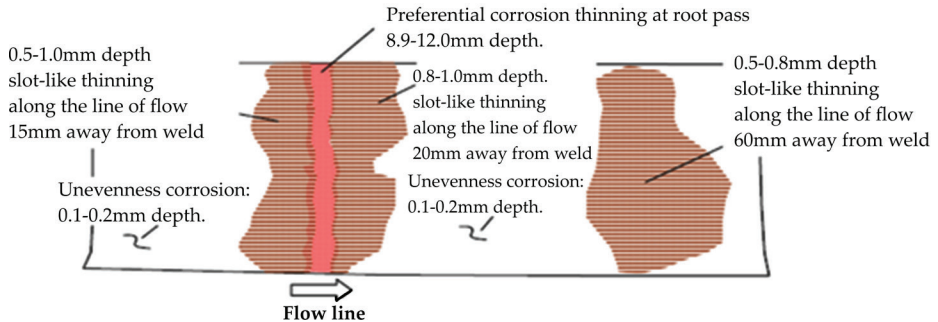


Figure 1: The internal surface condition of the pipeline

### 3.2 Microstructural Analysis Using Optical Microscope

Grain-refining region is produced when austenite grains decomposed into the ferrite and pearlite grain distribution during cooling owing to restricted diffusion moment [14]. Pearlite is an eutectoid mixture containing 0.80% carbon and is formed at 727 ° C when cooled very slowly [15]. It is a very fine plate like or lamellar mixture of ferrite and cementite. Partial grain-refining region prior pearlite colonies turn into austenite and expand upon heating moderately to previous ferrite, then decompose into highly fine pearlite and ferrite grains during cooling. Pearlite is a mixture of alternate strips of ferrite and cementite in a single grain as in Figure 2.

For microstructure of weld metal at upstream right side, pro-eutectoid ferrite forms along the austenite grain ferrite border when the weld metal is cooled in the austenite phase – ferrite transformation. In addition, polygon ferrite was also observed in the austenite grains in the form of coarse ferrite islands. Its presence reduces weld metal's toughness. With the increase in weld metal's carbon and chromium content, its amount decreases. Its quantity rises as heat input rises during welding and reduces as the weld metal's carbon and chromium content rises (Figure 3).

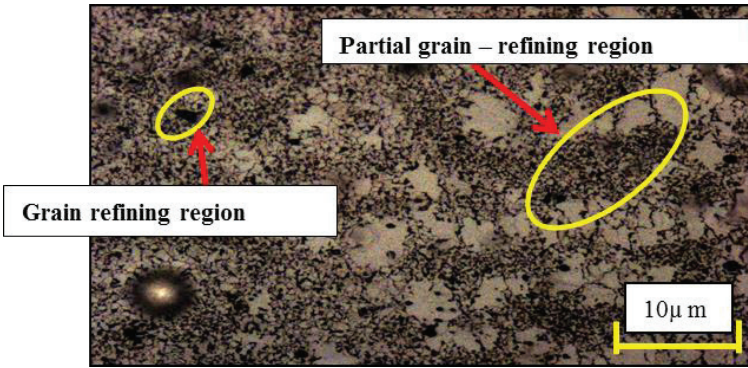


Figure 2: Microstructure of HAZ parent at upstream (right side)

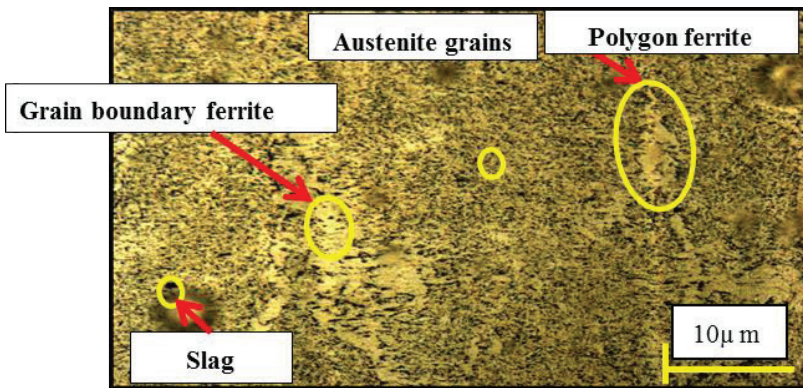
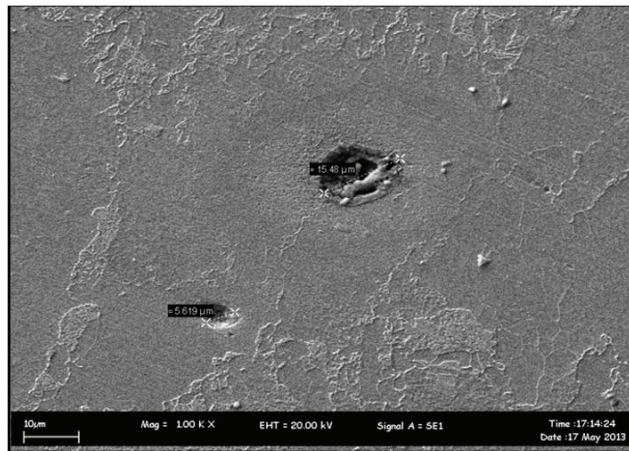


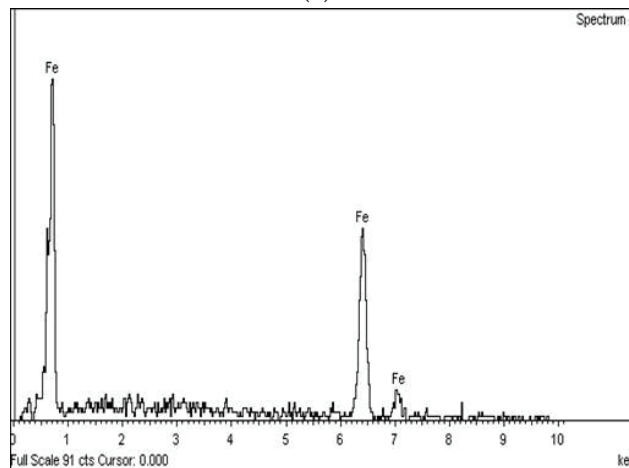
Figure 3: Microstructure of weld upstream (right side)

### 3.3 Observation Using Scanning Electron Microscope

The examination was conducted on scale of 10- $\mu$ m with magnification of 1000 X, pitting have been observed at 2 points at HAZ area (Figure 4 (a)). The diameter of pitting A is 5.62  $\mu$ m and porosity B is 15.48  $\mu$ m, respectively. Pitting was confirmed by EDX result where only Fe element exists at the peak of the graph as shown in Figure 4 (b).



(a)



(b)

Figure 4: (a) SEM image and (b) EDX result of pipeline sample at HAZ upstream

### 3.4 Vickers Hardness Testing

Figure 5 shows the hardness distribution of Vickers hardness testing. This pipe has served in severe condition where natural gas consist the most corrosive elements like carbon dioxide ( $\text{CO}_2$ ) and hydrogen sulfide ( $\text{H}_2\text{S}$ ), flowing inside the pipe system [16]. Additionally, the parent metal sustained the localized corrosion which related to the service temperature, conductivity of the corrosive element as well as thickness of the corrosive film in contact with metal has influence the parent metal properties to become erratic manner. Other factors that influence the changing of hardness distribution at parent metal is temperature ranging from ambient from welding to melting point.

Metallurgical transformations also happen during the process of preheat, fusion welding and effects due to multipass welding. Microstructure can significantly alter the intrinsic corrosion rate and as well as modified structure during cooling process induce to less efficiency of material properties.

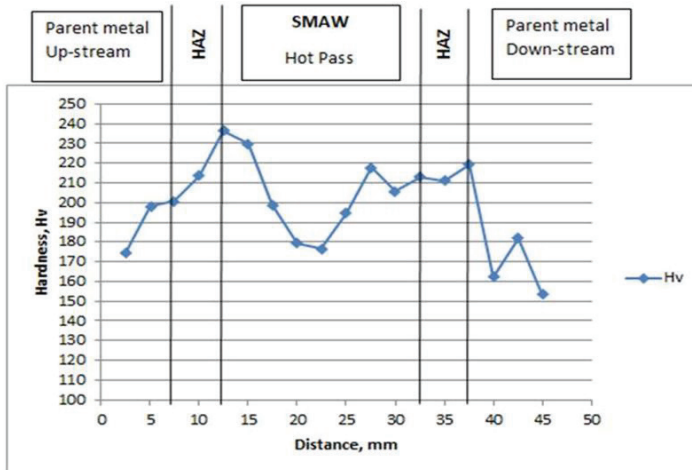


Figure 5: Hardness distribution of samples at different areas

At HAZ, ferrite supplied the welds with excellent mechanical characteristics such as tensile strength due to the greater resistance to crack propagation of its microstructure with fine size. A microstructure of acicular ferrite that was growing at inclusion was also observed. This has given the hardness of HAZ is very high compared with base and weld metal. But there was a decreasing value at HAZ (left side). This is due to the existence of polygonal ferrite which its presence reduces the strength of the weld metal. Factor that contribute to the amount of this microstructure increase, when increasing the heat input during welding, and due to high carbon and chromium content supply by welding electrode in manufacturing.

Based on the metallography examination by using OM, the microstructure in the weld area was polygon ferrite. The presence of this microstructure reduces the toughness, same as in HAZ microstructure at location downstream (left side). The amount of microstructure increases due to the increase in heat input during welding. It also reduces with the rise in weld metal's carbon and chromium content, which is usually added by welding electrode. The microstructures in this weld metal are grain boundary ferrite and coarse grain structure or grain coarsening region. High heat input and low cooling rate lead in a region of grain coarsening, resulting in low

hardness, lower tensile strength, yield strength and ductile welding [17]. This has proved that the existence of polygon ferrite and grain coarsening region microstructure in this shielded metal arc welding (SMAW), result to low hardness value during this Vickers hardness testing [18]. And this is suggested to be caused by high heat input and low cooling rate.

#### **4.0 CONCLUSION**

As a conclusion, the primary or root cause of the failure at weldment in carbon steel pipe was comprehended. The preference for weld corrosion was the primary root cause of this failure analysis of the weld region in the inner layer of the carbon steel pipeline. Through visual inspection and metallographic observations, theoretically the weld metal was anodic to HAZ and parent metal, then metal loss take place in weld metal. The result from OM revealed all the type and behaviors on microstructure which can influence the cause of the failure. Examination through SEM have revealed the discontinuity in weld metal and Vickers Hardness Testing shows the mechanical properties of each regions, at once all the findings can be related to the failure mechanism of the part.

#### **ACKNOWLEDGMENTS**

The authors would like to acknowledge Universiti Teknikal Malaysia Melaka for the experimental support and JX Nippon Oil and Gas Malaysia for supplying the pipe samples.

#### **REFERENCES**

- [1] P. Mayr, C. Schlacher, J.A. Siefert and J.D. Parker, "Microstructural features, mechanical properties and high temperature failures of ferritic to ferritic dissimilar welds", *International Materials Reviews*, vol. 64, no. 1, pp. 1-26, 2019.
- [2] R. Heidersbach, *Metallurgy and corrosion control in oil and gas production*. New Jersey: John Wiley & Sons, 2018.
- [3] M.A. Azam, S. Sukarti and M. Zaimi, "Corrosion behavior of API-5L-X42 petroleum/natural gas pipeline steel in South China Sea and Strait of Melaka seawaters", *Engineering Failure Analysis*, vol. 115, pp. 1-8, 2020.

- [4] J.O. Aina, O.A. Ojo and M.C. Chaturvedi, "Enhanced laser weldability of an aerospace superalloy by thermal treatment", *Science and Technology of Welding and Joining*, vol. 24, no. 3, pp. 225-234, 2019.
- [5] J. Garg and K. Singh, "Slag recycling in submerged arc welding and its effects on the quality of stainless steel claddings", *Materials & Design*, vol. 108, pp. 689-698, 2016.
- [6] K.A. Reddy, "Non-destructive testing, evaluation of stainless steel materials", *Materials Today: Proceedings*, vol. 4, no. 8, pp. 7302-7312, 2017.
- [7] D. Arsić, N. Gnjatović, S. Sedmak, A. Arsić and M. Uhričik, "Integrity assessment and determination of residual fatigue life of vital parts of bucket-wheel excavator operating under dynamic loads", *Engineering Failure Analysis*, vol. 105, pp.182-195, 2019.
- [8] E.A.S. Marques, R.J.C. Carbas, F. Silva, L.F. da Silva, D.P.S. de Paiva and F.D. Magalhães, "Use of master curves based on time-temperature superposition to predict creep failure of aluminium-glass adhesive joints", *International Journal of Adhesion and Adhesives*, vol. 74, pp. 144-154, 2017.
- [9] O. Ndubuaku, M. Martens, J.J. Cheng and S. Adeeb, "Integrating the shape constants of a novel material stress-strain characterization model for parametric numerical analysis of the deformational capacity of high-strength x80-grade steel pipelines", *Applied Sciences*, vol. 9, no. 2, pp. 322-345, 2019.
- [10] M. Sun and J.A. Packer, "Hot-dip galvanizing of cold-formed steel hollow sections: a state-of-the-art review", *Frontiers of Structural and Civil Engineering*, vol. 13, no. 1, pp. 49-65, 2019.
- [11] M. Mehdikhani, M. Aravand, B. Sabuncuoglu, M.G. Callens, S.V. Lomov and L. Gorbatikh, "Full-field strain measurements at the micro-scale in fiber-reinforced composites using digital image correlation", *Composite Structures*, vol. 140, pp. 192-201, 2016.
- [12] X. Jiang, N. Overman, N. Canfield and K. Ross, "Friction stir processing of dual certified 304/304L austenitic stainless steel for improved cavitation erosion resistance", *Applied Surface Science*, vol. 471, pp. 387-393, 2019.
- [13] M. Cabrini, S. Lorenzi, C. Testa, F. Brevi, S. Biamino, P. Fino, D. Manfredi, G. Marchese, F. Calignano and T. Pastore, "Microstructure and selective corrosion of alloy 625 obtained by means of laser powder bed fusion", *Materials*, vol. 12, no. 11, pp. 1-11, 2019.

- [14] B.S. Yilbas, S.S. Akhtar, C. Karatas and K. Boran, "Laser treatment of dual matrix cast iron with presence of WC particles at the surface: Influence of self-annealing on stress fields", *Optics & Laser Technology*, vol. 76, pp. 6-18, 2016.
- [15] J. Hidalgo, C. Celada-Casero and M.J. Santofimia, "Fracture mechanisms and microstructure in a medium Mn quenching and partitioning steel exhibiting macrosegregation", *Materials Science and Engineering: A*, vol. 754, pp. 766-777, 2019.
- [16] B.F. Pérez-Ramírez, A. Cervantes-Tobón, A. Ezeta-Mejía, S.J. García-Núñez and M. Díaz-Cruz, "Study of flow-assisted corrosion (FAC) in a API 5L X-70 steel in a brine-H<sub>2</sub>S-CO<sub>2</sub> system using the rotating cylindrical electrode", *Materials Research Express*, vol. 6, no. 6, pp. 1-19, 2019.
- [17] M.V.L. Ramesh, P.S. Rao, V.V. Rao and K.P. Prabhakar, "Structure-properties evaluation in laser beam welds of high strength low alloy steel", *Materials Today: Proceedings*, vol. 2, no. 4-5, pp. 2532-2537, 2015.
- [18] N.G. Chaidemenopoulos, P.P. Psyllaki, E. Pavlidou and G. Vourlias, "Aspects on carbides transformations of Fe-based hardfacing deposits", *Surface and Coatings Technology*, vol. 357, pp. 651-661, 2019.

